Cureus
Part of SPRINGER NATURE

Open Access Original Article

Shakuyaku-Kanzo-To Prevents Angiotensin II-Induced Cardiac Hypertrophy in Neonatal Rat Ventricular Myocytes

Review began 11/07/2024
Review ended 11/14/2024
Published 11/20/2024

DOI: 10.7759/cureus.74064

Hideaki Tagashira [1], Fumiha Abe [2], Ayako Sakai [2], Tomohiro Numata [1]

1. Department of Integrative Physiology, Akita University Graduate School of Medicine, Akita, JPN 2. Department of Integrative Physiology, Graduate School of Medicine, Akita University, Akita, JPN

Corresponding author: Tomohiro Numata, numata@med.akita-u.ac.jp

Abstract

The global incidence of mortality due to heart failure (HF) is on the rise, presenting a significant challenge in various regions, including Japan. There is an urgent need for innovative prevention and treatment strategies to address this issue. Traditional medicine, particularly Japanese Kampo medicine (JKM), has been proposed as a potential therapeutic approach and has undergone examination in clinical trials related to HF. However, the deficiency of robust scientific evidence underscores the necessity for further exploration into the cardioprotective mechanisms of JKM. This study systematically examines the cardioprotective effects of Shakuyaku-kanzo-to (SKT), a specific JKM with limited application in cardiac care. Utilizing neonatal rat ventricular myocytes, we assessed the direct effects of SKT on myocardial hypertrophy. Methodologies included immunohistochemistry for cell size and a plate reader for quantifying cell survival, intracellular calcium levels ($[Ca^{2+}]_i$), and reactive oxygen species (ROS) production. In addition, quantitative reverse transcription polymerase chain reaction (RT-PCR) was employed for gene expression analysis. The findings reveal that SKT significantly mitigates angiotensin **II** (Ang**II**)-induced cardiomyocyte hypertrophy and cell death, while also reducing elevated $[Ca^{2+}]_i$ and ROS production associated with this condition. Furthermore, co-administration of nifedipine, an L-type Ca^{2+} channel (L-Ca^{2+}) blocker, demonstrated that SKT antagonizes L-Ca^{2+} actions. These results indicate that SKT offers protection against Ang**II**-induced cardiomyocyte hypertrophy by inhibiting L-Ca^{2+}-mediated pathways. Consequently, this research highlights the potential of SKT as a promising therapeutic agent for cardiac applications, paving the way for new preventive and treatment strategies for HF.

Categories: Pharmacology, Integrative/Complementary Medicine, Cardiac/Thoracic/Vascular Surgery
Keywords: cardiomyocyte hypertrophy, japanese kampo medicine, l-type ca2+ channel, ros, shakuyaku-kanzo-to

Introduction

Cardiovascular diseases, such as myocardial hypertrophy and heart failure (HF), pose significant challenges to global health, characterized by considerable morbidity and mortality rates [1]. Among the various factors contributing to cardiovascular pathologies, dysregulation of intracellular calcium (Ca^{2+}) signaling and excessive production of reactive oxygen species (ROS) are recognized as critical mediators of cardiomyocyte hypertrophy and injury [2,3].

Among this dysregulation, angiotensin **II** (Ang**II**) is a crucial element of the renin-angiotensin system that plays a significant role in the induction of cardiomyocyte hypertrophy and cell death. This occurs through its effects on intracellular Ca^{2+} homeostasis and the production of ROS. In light of the advancements in pharmacological therapies, there has been an increasing interest in investigating the therapeutic potential of traditional herbal medicines, particularly regarding their ability to alleviate cardiovascular diseases [4,5]. In particular, Shakuyaku-kanzo-to (SKT), a traditional Japanese Kampo medicine, has been traditionally used to treat pain and muscle cramps [6,7]. Nonetheless, the specific effects of SKT on cardiac health, particularly regarding cardiomyocyte hypertrophy and cell death, have yet to be thoroughly explored. Given its prevalent use and potential therapeutic advantages, there is significant interest in investigating the cardioprotective properties of SKT.

In this study, we aimed to elucidate the effects of SKT on Ang**II**-induced cardiomyocyte hypertrophy and injury, focusing on its regulatory actions on intracellular Ca^{2+} signaling and ROS production. By employing neonatal rat ventricular myocytes (NRVMs) as an experimental model, we investigated the direct effects of SKT on cardiomyocytes and explored its underlying mechanisms of action.

Our findings provide valuable insights into the potential therapeutic utility of SKT in preventing Ang**II**-induced cardiomyocyte hypertrophy and cell death, thereby offering novel strategies for managing cardiovascular diseases. In addition, elucidating the mechanistic basis of SKT's cardioprotective effects may

pave the way for developing targeted therapeutic interventions for cardiovascular pathologies.

Materials And Methods

Materials

The Japanese Kampo medicine SKT (TJ-68) was obtained from Tsumura & Co. (Tokyo, Japan). The reagent was dissolved in dimethyl sulfoxide (DMSO) at a concentration of 250 mg/ml and subsequently diluted to the desired final concentration in aliquots. Ang**II** was purchased from Peptide Institute Inc. (Osaka, Japan). Nifedipine (NIF) was purchased from Sigma-Aldrich (MO, USA). Rhodamine-conjugated phalloidin was acquired from Abcam (ab235138, Abcam, Cambridge, UK). The ROS indicator, H_2DCFDA, was obtained from Invitrogen (Thermo Fisher Scientific, MA, USA), while the Ca^{2+} indicator, Fluo-4, was obtained from Dojindo Laboratories (Kumamoto, Japan). All other chemicals used in this study were guaranteed to be of reagent-grade quality, obtained from Nacalai Tesque, Inc. (Kyoto, Japan), Fujifilm Wako Pure Chemical Corp. (Osaka, Japan), and Sigma-Aldrich Co., LLC (St. Louis, MO, USA).

Animals

All animal experiments were conducted in strict adherence to the Guidelines for Care and Use of Laboratory Animals. Approval was obtained from the Animal Ethics Committee of Akita University, Japan, for a study period spanning from May 26, 2022, to May 25, 2025. The protocols were assigned ethics review numbers a-1-0412 and b-1-0408. Neonatal rats for the experiments were obtained from adult female Wistar rats (Japan SLC, Inc., Hamamatsu, Japan).

Cell culture

NRVMs were isolated from the hearts of Wistar rats aged one to three days. The rat pups were euthanized by decapitation by ethical guidelines. NRVMs were isolated using the Pierce Cardiomyocyte Isolation Kit (Thermo Fisher Scientific) following the provided protocol, as previously described [8]. Dispersed cells were cultured in Dulbecco's Modified Eagle Medium (DMEM; Sigma, D6429) supplemented with 10% fetal bovine serum (FBS) and penicillin/streptomycin (Nacalai Tesque, Kyoto, Japan) in a CO_2 incubator at 37°C.

Morphological analysis of NRVMs

The morphological analysis of NRVMs was conducted to assess the effects of 100 nM Ang**II** on cardiac hypertrophy, following established methodologies [8,9]. Cells fixed in 4% formaldehyde were stained with rhodamine-phalloidin (Abcam). The cross-sectional area (CSA) of the cells was quantified using fluorescence microscopy in conjunction with ImageJ software [10]. The 50% inhibitory concentration (IC_{50}) and Hill slope of SKT were calculated using GraphPad Prism 9 software (GraphPad Software, CA, USA) through a sigmoidal dose-response equation.

Measurement of cell viability and cytotoxicity

Cell viability and cytotoxicity were assessed using a colorimetric MTT assay (Cell Counting Kit-8, Dojindo) and an LDH activity assay (Cytotoxicity LDH Assay Kit-WST, Dojindo), respectively. NRVMs were plated at a density of 4.0×10^5 cells/mL in 96-well plates, cultured in DMEM, and treated with 100 nM AngII for 72 hours. Absorbance was measured at 450 nm for viability using a Multiskan JX plate reader (Thermo Fisher Scientific) and at 490 nm for cytotoxicity using an Infinite M200 microplate reader (Tecan Group Ltd.), with viability and cytotoxicity results presented as percentages relative to the control. Both assessments were conducted following previously established methodologies [8,11,12]. Cardiac cell hypertrophy was induced using 100 nM Ang**II** and cultured in 96-well plates. Briefly, SKT treatment was applied at a concentration of 500 µg/mL, as per the dosage used in previous studies on traditional herbal medicine, and was administered simultaneously with AngII [8].

Measurement of intracellular Ca^{2+} and ROS

Intracellular Ca^{2+} and ROS levels were measured in NRVMs following established protocols [8]. Cardiac cell hypertrophy was induced using 100 nM Ang**II**, and cells were subsequently cultured in 96-well plates. For the measurement of Ca^{2+}, Fluo-4 AM (F312, Dojindo) was utilized, while the measurement of ROS was performed using H_2DCFDA (C400, Invitrogen). Both fluorescent indicators were incubated with the cells for 30 minutes at 37°C in a CO_2 incubator, and fluorescence intensity at excitation/emission wavelength = 485/538 nm was quantified using a fluorescence microplate reader (Fluoroskan Ascent, Thermo Fisher Scientific).

RNA isolation and real-time RT-PCR

RNA isolation was conducted following a previously described protocol [8,13]. Total RNA was extracted from NRVMs utilizing the NucleoSpin® RNA Plus kit (Takara-Bio, Shiga, Japan) in accordance with the manufacturer's instructions. Reverse transcription of the total RNA samples was performed with the Prime-

Script™ II 1st strand cDNA Synthesis Kit (Takara-Bio). Quantitative real-time PCR was executed using the SYBR Green Real-Time PCR Master Mix-Plus (Toyobo Co., Ltd., Osaka, Japan) on a LightCycler® 480 System II (Roche Diagnostics Ltd., Rotkreuz, Switzerland). Gene-specific primers were synthesized by Sigma-Aldrich (MO, USA). The sequence for the rat primers employed was as follows (Table *1*).

Gene	Forward primer	Reverse primer	GeneBank accession #	Size (bp)	Reference
ANP	5'-AAATCCCGTATACAGTGCGG-3'	5'-GGAGGCATGACCTCATCTTC-3'	NM_012612.2	105	[8]
BNP	5'-CCATCGCAGCTGCCTGGCCCATCACTTCTG-3'	5'-GACTGCGCCGATCCGGTC-3'	NM_031545.1	364	[8]
Cav1.2	5'-CATTGCCTCCGAACACTA-3'	5'-GAACTTTCCACCAAACAGC-3'	NM_012517.2	412	[14]
β-actin	5'-ACTATCGGCAATGAGCGGTTC-3'	5'-ATGCCACAGGATTCCATACCC-3'	NM_031144.3	77	[8]

TABLE 1: Primer sequences used in PCR

ANP: atrial natriuretic peptide, BNP: brain natriuretic peptide, $Ca_v1.2$: L-type Ca^{2+} channel main subunit α1C; β-actin, PCR: polymerase chain reaction

Melting curve analysis was performed to affirm the specificity of the amplification. The relative expression levels of the target genes were normalized to the expression of the housekeeping gene β-actin using the ΔΔCt method. Furthermore, a representative gel image of the PCR products was captured using gel electrophoresis to confirm the specificity. PCR was conducted utilizing KOD-Plus-Ver.2 (Toyobo) as previously delineated [8]. The PCR products were separated on a 2% agarose gel and visualized using GelRedTM (Fujifilm Wako) staining.

Statistical analysis

Statistical analyses were performed utilizing GraphPad Prism software (version 9, GraphPad, San Diego, CA, USA). The results were presented as mean ± standard error of the mean (SEM). To evaluate the statistical significance between means, we applied Student's t-test following the verification of variance equality via an F-test. A p-value of less than 0.05 was deemed statistically significant. For multiple comparisons, one-way analysis of variance (ANOVA) was utilized, followed by Tukey's post-hoc test. To ensure the reproducibility of the results, the experiments were conducted a minimum of three times. The methodology for calculating the combination index (CI) was derived from a prior publication [15].

Results

SKT inhibits AngII-induced cardiomyocyte hypertrophy

AngII is widely recognized for its capacity to induce cardiomyocyte hypertrophy [16]. In order to evaluate the impact of SKT on hypertrophy and its associated cellular damage, a concentration of 100 nM of AngII was utilized [17,18].

After a 48-hour exposure to 100 nM AngII, a significant increase in cardiomyocyte hypertrophy was observed (Figure *1a*). The concentration of SKT applied in this study was 500 μg/ml, which was chosen based on literature indicating that concentrations of 100 μg/ml or higher are frequently employed in Kampo herbal medicine trials, with an effective range established between 250 and 500 μg/ml [13,19-28].

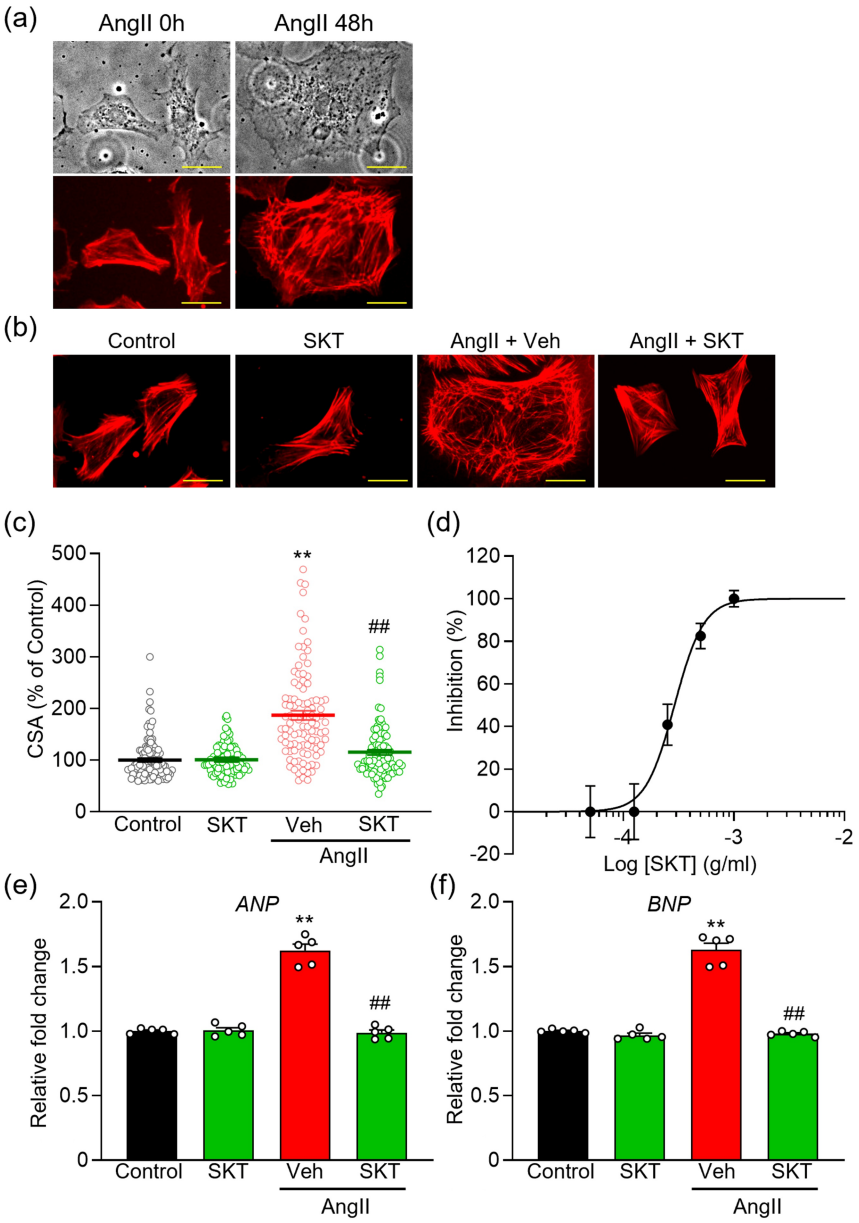

FIGURE 1: Effect of Shakuyaku-kanzo-to (SKT) on AngII-induced cardiomyocyte hypertorophy

(a) Representative cells are depicted in transmitted light images (top row) alongside rhodamine-conjugated phalloidin-stained fluorescence images (bottom row). NRVMs were characterized at 0 and 48 hours following the administration of Ang**II**. (b) Representative images of cells stained with rhodamine-conjugated phalloidin for each experimental group illustrate the effect of SKT (500 µg/ml) 48 hours after Ang**II** stimulation compared to the control group. (c) An evaluation of the antihypertrophic effect of SKT on Ang**II**-induced NRVM hypertrophy is presented through multiple cross-sectional area (CSA) measurements, as shown in panel (b). Each point represents one CSA measurement, and each group consists of >100 cells (n = 101-111). (d) Statistical analysis of the dose-dependent inhibition curve of SKT against Ang**II**-induced hypertrophy (n = 100-113). (e,f) Quantitative real-time PCR analysis of hypertrophic gene markers, ANP (e) and BNP (f) (n = 5). Each column represents the mean ± SEM.

, $p < 0.01$ indicates a significant difference compared to Control group. ##, $p < 0.01$ indicates a significant difference compared to AngII** + Veh group. Scale bar = 50 µm.

SKT: Shakuyaku-kanzo-to, Ang**II**: angiotensin **II**, NRVMs: neonatal rat ventricular myocytes, PCR: polymerase chain reaction, ANP: atrial natriuretic peptide, BNP: brain natriuretic peptide, SEM: standard error of the mean

The treatment with SKT did not produce a significant change in the cross-sectional area (CSA) of cardiomyocytes when compared to the control group (Figures *1b*, *1c*: Control, SKT) However, it did significantly reduce Ang**II**-induced cardiomyocyte hypertrophy (Figures *1b*, *1c*: Ang**II** + Veh, Ang**II** + SKT).

Furthermore, dose-dependent experiments demonstrated that SKT effectively inhibited AngII-induced hypertrophy, exhibiting an IC_{50} value of 290.3 µg/ml and a Hill slope of 3.3 (Figure *1d*).

To further clarify the impact of SKT on cardiac hypertrophy, we conducted quantitative reverse transcriptase polymerase chain reaction (qRT-PCR) experiments to assess the expression of key cardiac hypertrophic marker genes, specifically atrial natriuretic peptide (ANP) and brain natriuretic peptide (BNP). Our findings revealed a significant increase in the expression of these markers due to AngII-induced cardiomyocyte hypertrophy. Notably, treatment with SKT resulted in a marked reduction in their expression levels (Figure *1e*).

Protective effect of SKT against cell damage associated with AngII-induced hypertrophy

Subsequently, we investigated the potential protective effects of SKT against cell damage linked to AngII-induced hypertrophy. Our results demonstrated that SKT significantly mitigated the AngII-induced reduction in cell viability and the corresponding increase in cytotoxicity (Figure *2a*, *2b*: AngII + Veh, AngII + SKT). Furthermore, it is noteworthy that treatment with 500 µg/ml SKT alone did not result in any significant alterations in cell viability or cardiomyocyte toxicity when compared to control cells (Figures *2a*, *2b*: Control, SKT).

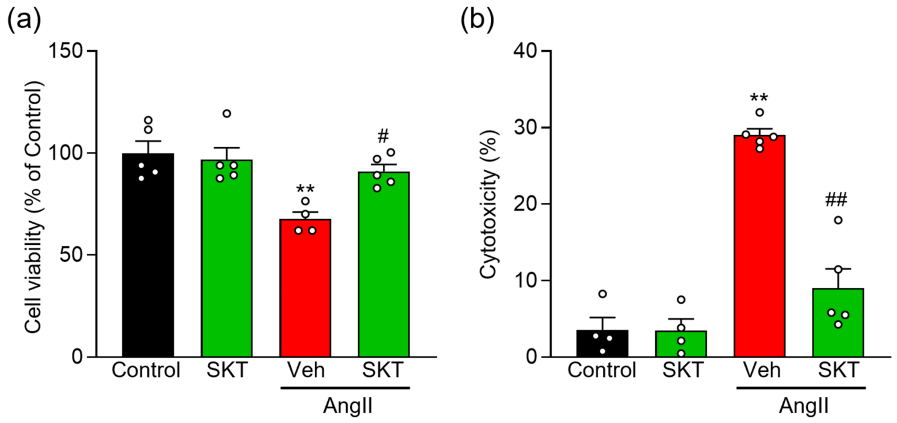

FIGURE 2: Effect of SKT on AngII-induced NRVMs cell death

Evaluation of the effect of SKT treatment on NRVMs after 48 h of AngII administration. NRVM were treated with either vehicle (Control or Veh) or 500 µg/ml SKT (SKT) with or without AngII induction. (a) The MTT assay assessed cell viability (n = 4-5). (b) Cytotoxicity was evaluated through LDH release assay (n = 4-5). Each column represents the mean ± SEM.

**, $p < 0.01$ indicates a significant difference compared to the control group. #, $p < 0.05$ and ##, $p < 0.01$ indicate significant differences compared to the AngII + Veh group.

SKT: Shakuyaku-kanzo-to, AngII: angiotensin II, NRVMs: neonatal rat ventricular myocytes, SEM: standard error of the mean

SKT attenuates AngII-induced abnormalities in intracellular Ca^{2+} and ROS levels

To investigate the myocardial protective mechanism of SKT, we examined the intracellular environment. It is widely recognized that cardiomyocyte hypertrophy and injury result from elevated intracellular Ca^{2+} and ROS levels [2,3]. Consequently, we sought to elucidate the cardioprotective effects of SKT by analyzing intracellular Ca^{2+} and ROS levels in NRVMs induced with AngII. Consistent with previous studies [8,29,30], our findings indicate that treatment with AngII for a duration of 48 hours resulted in a significant elevation in both intracellular Ca^{2+} and ROS levels (Figures *3a*, *3c*). By contrast, treatment with SKT markedly mitigated these AngII-induced increases in Ca^{2+} and ROS. Specifically, the AngII-induced elevation of intracellular Ca^{2+} was significantly diminished in the SKT treatment group in a dose-dependent manner, exhibiting an IC_{50} value of 8.6 µg/ml and a Hill slope of 1.1 (Figures *3a*, *3b*). Furthermore, ROS levels were similarly reduced in the SKT treatment group, demonstrating an IC_{50} of 5.4 µg/ml and a Hill slope of 0.9 (Figures *3c*, *3d*).

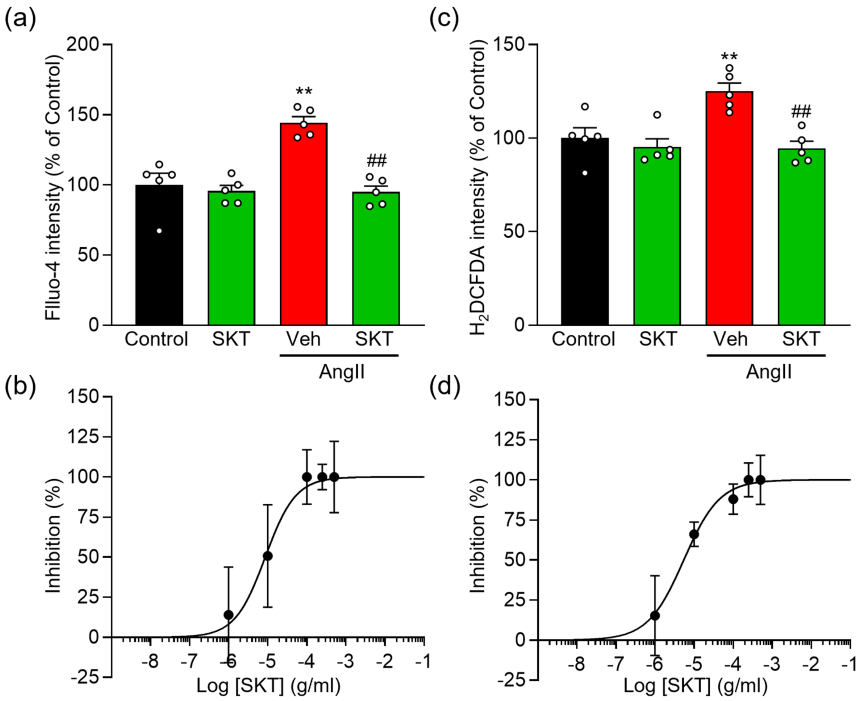

FIGURE 3: Effect of SKT on intracellular Ca2+ and ROS concentrations of AngII-induced NRVMs

Evaluation of the effect of SKT treatment on NRVM were treated with either vehicle (Control or Veh) or 500 μg/ml SKT (SKT) with or without Ang**II** induction. (a) Intracellular Ca^{2+} concentration was measured by Fluo-4 intensity (n = 5). (b) Statistical analysis of the dose-dependent inhibition curve of SKT against Ang**II**-induced intracellular Ca^{2+} elevation. (c) Intracellular ROS concentration was assessed through H_2DCFDA intensity (n = 5). (d) Statistical analysis of the dose-dependent inhibition curve of SKT against Ang**II**-induced increase in ROS production. Each column represents the mean ± SEM.

, $p < 0.01$ indicates a significant difference compared to the control group. ##, $p < 0.01$ indicates a significant difference compared to the AngII** + Veh group.

SKT: Shakuyaku-kanzo-to, ROS: reactive oxygen species, Ang**II**: angiotensin **II**, NRVMs: neonatal rat ventricular myocytes, SEM: standard error of the mean

These results underscore the potential of SKT in conferring protection against Ang**II**-induced cellular disturbances.

SKT improves Ang**II**-induced cardiomyocyte hypertrophy by acting on antagonistic targets to Nifedipine

It is well-established that the influx of Ca^{2+} through L-type Ca^{2+} channels (L-Ca^{2+}) play a crucial role in Ang**II**-induced cardiomyocyte hypertrophy [31]. To investigate this further, we examined the expression of the *CACNA1C* gene ($Ca_v1.2$), which encodes the primary α1C subunit responsible for forming L-Ca^{2+} in NRVMs. Results from RT-PCR indicated significant expression of $Ca_v1.2$ in NRVMs. Notably, this expression remained relatively unchanged at the mRNA level in both Ang**II**-induced and control NRVMs, regardless of SKT treatment (Figures *4a*, *4b*).

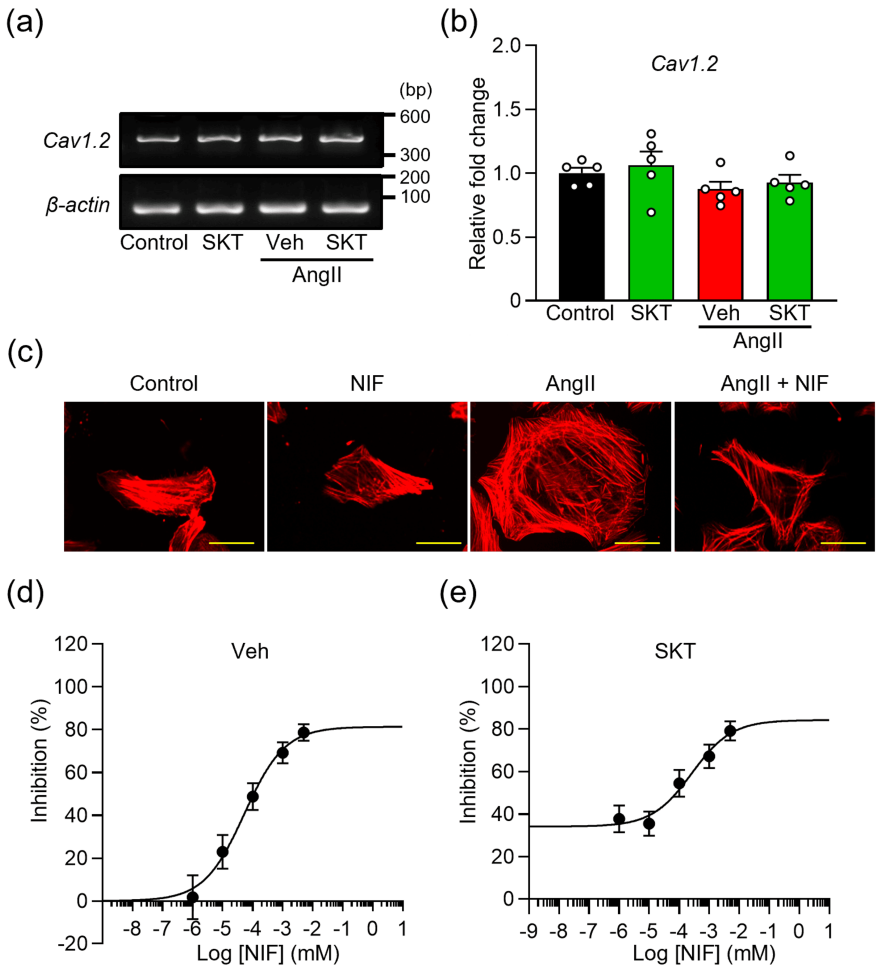

FIGURE 4: Effect of SKT on the L-type Ca2+ channel in AngII-induced cardiomyocyte hypertrophy

(a) mRNA expression of the CACNA1C gene encoding the L-type Ca^{2+} channel ($Ca_v1.2$). PCR products obtained from NRVMs treated with vehicle (Control or Veh), or 250 μg/ml SKT, after 48 hours of Ang**II**-induced cardiomyocyte hypertrophy show the expression of $Ca_v1.2$ and a constitutively transcribed control β-actin. (b) Quantitative real-time PCR analysis of $Ca_v1.2$ mRNA (n = 5). (c) Representative images of cells stained with rhodamine-conjugated phalloidin to investigate the effect of NIF (1 μM) on Ang**II**-induced cardiomyocyte hypertrophy. (d) Dose-dependent inhibition curve of NIF on Ang**II**-induced cardiomyocyte hypertrophy (n = 103-119). (e) Dose-dependent inhibition curve of NIF combined with 250 μg/ml SKT on Ang**II**-induced cardiomyocyte hypertrophy (n = 100-109). Each group consisted of more than 100 cells. Each column represents the mean ± SEM.

SKT: Shakuyaku-kanzo-to, Ang**II**: angiotensin **II**, PCR: polymerase chain reaction, NRVMs: neonatal rat ventricular myocytes, SEM: standard error of the mean

To assess the impact of L-Ca^{2+} on Ang**II**-induced NRVMs, we measured the CSA using NIF, a selective blocker of L-Ca^{2+}. The effects of NIF on cardiomyocyte hypertrophy exhibited a dose-dependent relationship, with an IC_{50} of 53.1 nM and a Hill slope of 0.6 (Figures *4c*, *4d*). Notably, 5 μM NIF was the maximum allowed due to cardiotoxicity observed at higher concentrations. These findings for the effects of NIF on NRVMs were consistent with previous studies involving cardiomyocytes [32-34].

Subsequently, we investigated to determine the combination index (CI) to elucidate the interaction of SKT with the NIF of the target. The concentration-dependent inhibition curve of NIF in the presence of 250 μg/ml SKT, which corresponds to approximately half the inhibitory effect of SKT calculated in Figure *1d*, demonstrated a significant effect at NIF concentrations of 0.01 μM or higher, with a CI of 1.2 (see Figure *4e*).

Moreover, treatment with SKT, or SKT and NIF, effectively suppressed the Ang**II**-induced increase in $[Ca^{2+}]_i$

and ROS production, with no significant differences noted in their inhibitory effects (Figure 5).

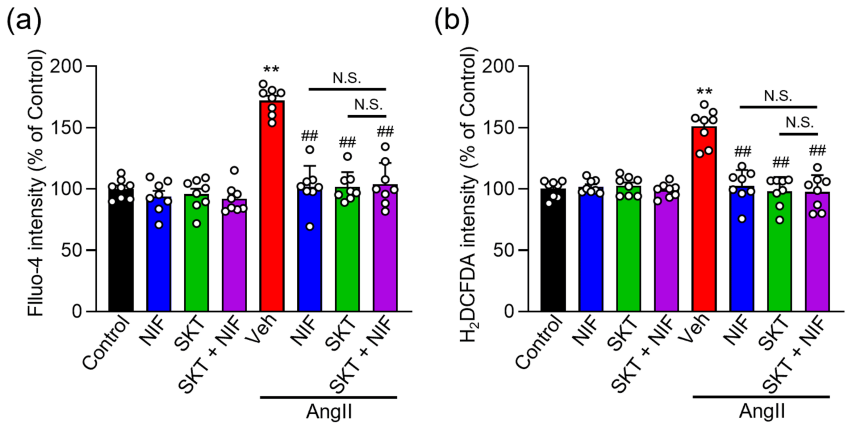

FIGURE 5: Impact of SKT on intracellular Ca2+ and ROS levels during AngII-induced cardiomyocyte hypertrophy in the presence of nifedipine

(a, b) The effects of 250 μg/ml SKT, 1 μM NIF, or 1 μM NIF and 250 μg/ml SKT, or vehicle (Control or Veh) in NRVMs with and without Ang**II** induction of cardiomyocyte hypertrophy for 48 h was assessed by observing intracellular Ca^{2+} concentration (Fluo-4 intensity) (n = 8) (a) and ROS production (H2DCFDA intensity) (n = 8-9) (b). Each column represents the mean ± SEM.

, $p < 0.01$ indicates a significant difference compared to Control group. ##, $p < 0.01$ indicates a significant difference compared to AngII** + Veh group. N.S. indicates no significant difference.

SKT: Shakuyaku-kanzo-to, Ang**II**: angiotensin **II**, ROS: reactive oxygen species, SEM: standard error of the mean

These results indicate that SKT inhibits the influx of Ca $^{2+}$ through L-Ca^{2+}, thereby suppressing the increase in intracellular Ca^{2+} levels and ROS production, contributing to the mitigation of Ang**II**-induced cardiomyocyte hypertrophy.

Discussion

This study aimed to investigate the impact of SKT on cardiomyocytes, with a primary focus on its potential to mitigate Ang**II**-induced hypertrophy and cell death. Our findings reveal, for the first time, that SKT exerts a direct effect on cardiomyocytes, effectively preventing Ang**II**-induced hypertrophy and subsequent cell death. In addition, SKT demonstrates protective properties against Ang**II**-induced disruption of intracellular Ca^{2+} homeostasis and ROS production. This is partly achieved by inhibiting Ca^{2+} influx through L-type Ca^{2+} channels, thereby contributing to its cardioprotective effects. Although the precise molecular mechanisms remain to be elucidated, our results suggest that SKT mitigates cardiomyocyte hypertrophy and injury by targeting the aberrant Ca^{2+} and ROS signaling pathways triggered by Ang**II**.

Clinical observations suggest that SKT may precipitate cardiac arrhythmias owing to alterations in serum potassium levels [35]. This underscores the necessity for vigilant monitoring of potassium concentrations during its administration. Notwithstanding this precaution, the primary conclusion of our study is that SKT significantly mitigates AngII-induced cardiomyocyte hypertrophy and injury, thereby demonstrating a direct protective effect on NRVMs. Indeed, clinical observations indicate that the administration of SKT contributes positively to improved mortality rates in patients suffering from diabetic cardiomyopathy [25].

SKT is a traditional Japanese herbal medicine formulation that combines licorice (*Glycyrrhizae Radix*) and peony (*Paeoniae Radix*) in a 1:1 ratio. Glycyrrhizic acid (GA) derived from licorice and peonyflorin (PF) from peony are recognized as its active components, both possessing cardioprotective properties. The inhibitory effect of SKT does not acutely target the L-type Ca^{2+} channel pore, but Ca^{2+} imaging analysis shows a decrease in cytoplasmic Ca^{2+} concentration [36]. This suggests a potential long-term inactivation mechanism involving internalization of L-type Ca^{2+} channels in cardiomyocytes [37]. In addition, there may be an indirect inhibitory effect mediated by sodium-calcium exchanger (NCX), calcium pumps, and background calcium leak [38]. Further studies are required to confirm these possible mechanisms.

GA, a triterpenoid saponin found in licorice roots, is known to influence metabolic regulation. The cardioprotective effects of GA and its aglycones have been documented in various models [39], including pressure overload-induced cardiac hypertrophy and isoproterenol-induced ischemic injury [40,41]. Supportive evidence from studies conducted by Yasuda and Kanzaki indicates that highly lipophilic

components from licorice, including GA, exhibit inhibitory effects on smooth muscle contraction in uterine tissues [22,23,26]. The L-type Ca^{2+} channel appears to be a critical route involved in this process [42]. In our study, we utilized cultured cardiomyocytes to induce hypertrophy via Ang**II** stimulation, which triggers Ca^{2+} influx through L-type Ca^{2+} channels [31]. Notably, our combination index results indicated that SKT mitigated the effects of Ang**II** stimulation in NRVMs by counteracting the inhibitory effects of NIF, a selective inhibitor of L-type Ca^{2+} channels (Figure *4e*). Furthermore, SKT nearly completely inhibited Ang**II**-induced cardiac hypertrophy, whereas NIF provided only partial inhibition (Figures *1d*, *4d*). These findings robustly suggest that SKT confers its cardioprotective effects through multiple mechanisms.

PF, a constituent of peonies, has garnered attention for its cardioprotective effects. It has been shown to protect against various heart diseases by suppressing ROS production. For example, PF protects against myocardial ischemia and reperfusion injuries in rats [43-49], heart failure in lipopolysaccharides (LPS)- or cecal ligation and puncture (CLP)-induced sepsis in mice and rats, and cardiac injury in response to coronary artery ligation-induced pressure overload in mice and rats [50-55]. It has been proposed that the protective effects of PF operate through the suppression of inflammatory cytokine production by inhibiting ROS and affecting the inducible nitric oxide synthase (iNOS) signaling pathway [53,55,56]. In models of diabetes-induced myocardial infarction and isoproterenol-induced chronic heart failure, PF appears to protect the heart through mechanisms that do not involve regulating Ca^{2+} influx. Rather, it downregulates the TRPV1/CaMK/CREB/CGRP and TGF-β1/Smad signaling pathways, providing protection against myocardial infarction and fibrosis [57-59]. In addition, PF pretreatment in H9c2 cells has been observed to inhibit apoptosis induced by doxorubicin, acrolein, and Ang**II** by reducing ROS production [60-62]. These findings indicate that PF might engage in protective mechanisms against heart disease through multiple pathways, thus sustaining and enhancing cardiac functions. Its mechanisms span from cellular to organ levels, with a primary focus on cardiac protection and reduction of ROS. Our findings demonstrated the suppression of Ang**II**-induced ROS and consequent cell damage (Figures *2*, *3c*, b), aligning with prior research. It is anticipated that PF's presence in Paeonia contributes to the inhibition of cell death in myocardial hypertrophic cells by reducing ROS levels.

The combined presence of GA and PF in SKT has demonstrated an inhibitory effect on smooth muscle contraction, with an IC_{50} of approximately 440 μg/ml, as evidenced in a study conducted on human uterine tissue [26]. This finding closely aligns with our observations regarding the inhibition of cardiac hypertrophy in cardiomyocytes (Figure *1c*).

This study acknowledges several limitations. First, since cultured cardiomyocytes were utilized, further verification through animal models and clinical trials is essential. Moreover, while it has been observed that SKT operates via voltage-gated L-type Ca^{2+} channels, additional research is necessary to investigate its effects on other calcium channel types and calcium-related factors. Furthermore, previous reports indicate that SKT may induce cardiac arrhythmias, necessitating vigilant management of potassium concentrations during clinical application, which represents another limitation to consider. Lastly, although GA and PF are recognized as the primary active ingredients of SKT, a comprehensive analysis is crucial to elucidate the role of other compounds and to ascertain whether the cardioprotective effects result from the specific combinations and quantitative ratios of these compounds.

Conclusions

This study highlights the potential of SKT as a therapeutic intervention for cardiovascular conditions characterized by cardiomyocyte hypertrophy and apoptosis. SKT demonstrates cardioprotective properties that may involve modulation of calcium channels and downstream signaling pathways, which could be beneficial in mitigating harmful effects associated with Ang**II**-induced cardiac stress. These findings contribute to understanding the pharmacological actions of SKT and underscore its therapeutic promise in managing cardiac hypertrophy and cell death.

Additional Information

Author Contributions

All authors have reviewed the final version to be published and agreed to be accountable for all aspects of the work.

Concept and design: Tomohiro Numata, Hideaki Tagashira

Acquisition, analysis, or interpretation of data: Tomohiro Numata, Ayako Sakai, Fumiha Abe, Hideaki Tagashira

Drafting of the manuscript: Tomohiro Numata

Critical review of the manuscript for important intellectual content: Tomohiro Numata, Ayako Sakai, Fumiha Abe, Hideaki Tagashira

Supervision: Tomohiro Numata

Disclosures

Human subjects: All authors have confirmed that this study did not involve human participants or tissue. **Animal subjects:** Animal Ethics Committee of Akita University (Akita, Japan) Issued protocol number a-1-0412 and b-1-0408. **Conflicts of interest:** In compliance with the ICMJE uniform disclosure form, all authors declare the following: **Payment/services info:** This research was partially supported by the following grants and funding sources: JSPS KAKENHI Grant (22K06659, 22K06659DK H.T., and 21K06792 T.N.); Funding for Advanced Research by the Dean of the Graduate School of Medicine, Akita University (H.T.), Kobayashi Foundation (H.T.), Nishinomiya Basic Research Fund (H.T.), Akita Prefecture Technology Innovation Creation and Utilization Promotion Project (H.T.); and Japan Kampo Medicine Education Foundation grant number 2023 (T.N.). In addition, support was provided by JKA and its promotion funds from KEIRIN RACE (T.N.). **Financial relationships:** All authors have declared that they have no financial relationships at present or within the previous three years with any organizations that might have an interest in the submitted work. **Other relationships:** All authors have declared that there are no other relationships or activities that could appear to have influenced the submitted work.

References

1. Roger VL: Epidemiology of heart failure. Circ Res. 2013, 113:646-59. 10.1161/CIRCRESAHA.113.300268
2. Bertero E, Maack C: Calcium signaling and reactive oxygen species in mitochondria. Circ Res. 2018, 122:1460-78. 10.1161/CIRCRESAHA.118.310082
3. Bers DM: Altered cardiac myocyte Ca regulation in heart failure. Physiology (Bethesda). 2006, 21:380-7. 10.1152/physiol.00019.2006
4. Yaku H, Kaneda K, Kitamura J, Kato T, Kimura T: Kampo medicine for the holistic approach to older adults with heart failure. J Cardiol. 2022, 80:306-12. 10.1016/j.jjcc.2021.12.011
5. Ezaki H, Ayaori M, Sato H, Maeno Y, Taniwaki M, Miyake T, Sakurada M: Effects of Mokuboito, a Japanese Kampo medicine, on symptoms in patients hospitalized for acute decompensated heart failure - a prospective randomized pilot study. J Cardiol. 2019, 74:412-7. 10.1016/j.jjcc.2019.05.003
6. Sadakane C, Watanabe J, Fukutake M, Nisimura H, Maemura K, Kase Y, Kono T: Pharmacokinetic profiles of active components after oral administration of a Kampo medicine, shakuyakukanzoto, to healthy adult Japanese volunteers. J Pharm Sci. 2015, 104:3952-9. 10.1002/jps.24596
7. Hinoshita F, Ogura Y, Suzuki Y, et al.: Effect of orally administered shao-yao-gan-cao-tang (Shakuyaku-kanzo-to) on muscle cramps in maintenance hemodialysis patients: a preliminary study. Am J Chin Med. 2003, 31:445-53. 10.1142/S0192415X03001144
8. Tagashira H, Abe F, Sato-Numata K, et al.: Cardioprotective effects of Moku-boi-to and its impact on AngII-induced cardiomyocyte hypertrophy. Front Cell Dev Biol. 2023, 11:1264076. 10.3389/fcell.2023.1264076
9. Tagashira H, Bhuiyan MS, Shioda N, Fukunaga K: Fluvoxamine rescues mitochondrial Ca2+ transport and ATP production through σ(1)-receptor in hypertrophic cardiomyocytes. Life Sci. 2014, 95:89-100. 10.1016/j.lfs.2013.12.019
10. Schneider CA, Rasband WS, Eliceiri KW: NIH Image to ImageJ: 25 years of image analysis. Nat Methods. 2012, 9:671-5. 10.1038/nmeth.2089
11. Numata T, Sato K, Okada Y, Wehner F: Hypertonicity-induced cation channels rescue cells from staurosporine-elicited apoptosis. Apoptosis. 2008, 13:895-903. 10.1007/s10495-008-0220-y
12. Tagashira H, Bhuiyan MS, Shinoda Y, Kawahata I, Numata T, Fukunaga K: Sigma-1 receptor is involved in modification of ER-mitochondria proximity and Ca(2+) homeostasis in cardiomyocytes. J Pharmacol Sci. 2023, 151:128-33. 10.1016/j.jphs.2022.12.005
13. Numata T, Sato-Numata K, Okada Y, Inoue R: Cellular mechanism for herbal medicine Junchoto to facilitate intestinal Cl(-)/water secretion that involves cAMP-dependent activation of CFTR. J Nat Med. 2018, 72:694-705. 10.1007/s11418-018-1207-9
14. Wang R, Ma Z, Wang J, Xie J: L-type Cav1.2 calcium channel is involved in 6-hydroxydopamine-induced neurotoxicity in rats. Neurotox Res. 2012, 21:266-70. 10.1007/s12640-011-9271-x
15. Chou TC: Drug combination studies and their synergy quantification using the Chou-Talalay method. Cancer Res. 2010, 70:440-6. 10.1158/0008-5472.CAN-09-1947
16. Sadoshima J, Izumo S: Molecular characterization of angiotensin II--induced hypertrophy of cardiac myocytes and hyperplasia of cardiac fibroblasts. Critical role of the AT1 receptor subtype. Circ Res. 1993, 73:413-23. 10.1161/01.res.73.3.413
17. Huang CY, Kuo WW, Yeh YL, et al.: ANG II promotes IGF-IIR expression and cardiomyocyte apoptosis by inhibiting HSF1 via JNK activation and SIRT1 degradation. Cell Death Differ. 2014, 21:1262-74. 10.1038/cdd.2014.46
18. Li J, Qi M, Li C, et al.: Tom70 serves as a molecular switch to determine pathological cardiac hypertrophy. Cell Res. 2014, 24:977-93. 10.1038/cr.2014.94
19. Kakimoto M, Nomura T, Nazmul T, et al.: In vitro Suppression of SARS-CoV-2 Infection by Existing Kampo Formulas and Crude Constituent Drugs Used for Treatment of Common Cold Respiratory Symptoms. Front Pharmacol. 2022, 13:804103. 10.3389/fphar.2022.804103
20. Numata T, Sato-Numata K, Okada Y: Herbal components of Japanese Kampo medicines exert laxative actions in colonic epithelium cells via activation of BK and CFTR channels. Sci Rep. 2019, 9:15554. 10.1038/s41598-019-52171-z
21. Suganami A, Sakamoto K, Ono T, Watanabe H, Hijioka N, Murakawa M, Kimura J: The inhibitory effect of shakuyakukanzoto on K+ current in H9c2 cells. Fukushima J Med Sci. 2014, 60:22-30. 10.5387/fms.2013-16
22. Sumi G, Yasuda K, Kanamori C, et al.: Two-step inhibitory effect of kanzo on oxytocin-induced and prostaglandin F2α-induced uterine myometrial contractions. J Nat Med. 2014, 68:550-60. 10.1007/s11418-

014-0835-y
23. Sumi G, Yasuda K, Tsuji S, et al.: Lipid-soluble fraction of Shakuyaku-kanzo-to inhibits myometrial contraction in pregnant women. J Obstet Gynaecol Res. 2015, 41:670-9. 10.1111/jog.12618
24. Takeuchi A, Koga K, Tokita Y, et al.: The effects of tokishakuyakusan, a traditional Japanese medicine (kampo), ferulic acid and paeoniflorin, on human endometriotic stromal cells and peritoneal macrophages. J Reprod Immunol. 2020, 139:103104. 10.1016/j.jri.2020.103104
25. Tsai FJ, Ho TJ, Cheng CF, et al.: Characteristics of Chinese herbal medicine usage in ischemic heart disease patients among type 2 diabetes and their protection against hydrogen peroxide-mediated apoptosis in H9C2 cardiomyoblasts. Oncotarget. 2017, 8:15470-89. 10.18632/oncotarget.14657
26. Tsuji S, Yasuda K, Sumi G, Cho H, Tsuzuki T, Okada H, Kanzaki H: Shakuyaku-kanzo-to inhibits smooth muscle contractions of human pregnant uterine tissue in vitro. J Obstet Gynaecol Res. 2012, 38:1004-10. 10.1111/j.1447-0756.2011.01827.x
27. Zhang Q, Guo D, Wang Y, et al.: Danqi pill protects against heart failure post-acute myocardial infarction via HIF-1α/PGC-1α mediated glucose metabolism pathway. Front Pharmacol. 2020, 11:458. 10.3389/fphar.2020.00458
28. Zhang Q, Shao M, Zhang X, et al.: The effect of Chinese medicine on lipid and glucose metabolism in acute myocardial infarction through pparγ pathway. Front Pharmacol. 2018, 9:1209. 10.3389/fphar.2018.01209
29. Zhao GJ, Zhao CL, Ouyang S, et al.: Ca(2+)-dependent NOX5 (NADPH oxidase 5) exaggerates cardiac hypertrophy through reactive oxygen species production. Hypertension. 2020, 76:827-38. 10.1161/HYPERTENSIONAHA.120.15558
30. Wang S, Han HM, Pan ZW, et al.: Choline inhibits angiotensin II-induced cardiac hypertrophy by intracellular calcium signal and p38 MAPK pathway. Naunyn Schmiedebergs Arch Pharmacol. 2012, 385:823-31. 10.1007/s00210-012-0740-4
31. Aiello EA, Cingolani HE: Angiotensin II stimulates cardiac L-type Ca(2+) current by a Ca(2+)- and protein kinase C-dependent mechanism. Am J Physiol Heart Circ Physiol. 2001, 280:H1528-36. 10.1152/ajpheart.2001.280.4.H1528
32. Ago T, Yang Y, Zhai P, Sadoshima J: Nifedipine inhibits cardiac hypertrophy and left ventricular dysfunction in response to pressure overload. J Cardiovasc Transl Res. 2010, 3:304-13. 10.1007/s12265-010-9182-x
33. Bedut S, Seminatore-Nole C, Lamamy V, et al.: High-throughput drug profiling with voltage- and calcium-sensitive fluorescent probes in human iPSC-derived cardiomyocytes. Am J Physiol Heart Circ Physiol. 2016, 311:H44-53. 10.1152/ajpheart.00793.2015
34. Hotchkiss A, Feridooni T, Zhang F, Pasumarthi KB: The effects of calcium channel blockade on proliferation and differentiation of cardiac progenitor cells. Cell Calcium. 2014, 55:238-51. 10.1016/j.ceca.2014.02.018
35. Yoshino T, Shimada S, Homma M, Makino T, Mimura M, Watanabe K: Clinical risk factors of licorice-induced pseudoaldosteronism based on glycyrrhizin-metabolite concentrations: a narrative review. Front Nutr. 2021, 8:719197. 10.3389/fnut.2021.719197
36. Tasaki K, Noble PJ, Garny A, Shorten PR, Afshar N, Noble D: Model of skeletal muscle cramp and its reversal . Physiome. 2021, 10.36903/physiome.12885590
37. Hermosilla T, Encina M, Morales D, et al.: Prolonged AT(1)R activation induces Ca(V)1.2 channel internalization in rat cardiomyocytes. Sci Rep. 2017, 7:10131. 10.1038/s41598-017-10474-z
38. Noble PJ, Garny A, Shorten PR, Tasaki K, Afshar N, Noble D: Incorporation of sarcolemmal calcium transporters into the Shorten et al. (2007) model of skeletal muscle: equations, coding and stability. Physiome. 2020, 10.36903/physiome.12885590.v2
39. Cheng X, Huang L: The mechanism of the anti-cardiac hypertrophy effect of glycyrrhizic acid is related to reducing STIM1-dependent store-operated calcium entry. Bull Exp Biol Med. 2023, 174:701-6. 10.1007/s10517-023-05774-6
40. Zhao Z, Liu M, Zhang Y, et al.: Cardioprotective effect of monoammonium glycyrrhizinate injection against myocardial ischemic injury in vivo and in vitro: involvement of inhibiting oxidative stress and regulating Ca(2+) homeostasis by L-type calcium channels. Drug Des Devel Ther. 2020, 14:331-46. 10.2147/DDDT.S232130
41. Li M, Wen Z, Xue Y, et al.: Cardioprotective effects of glycyrrhizic acid involve inhibition of calcium influx via L-type calcium channels and myocardial contraction in rats. Naunyn Schmiedebergs Arch Pharmacol. 2020, 393:979-89. 10.1007/s00210-019-01767-3
42. Wray S, Arrowsmith S: Uterine excitability and ion channels and their changes with gestation and hormonal environment. Annu Rev Physiol. 2021, 83:331-57. 10.1146/annurev-physiol-032420-035509
43. Chen H, Dong Y, He X, Li J, Wang J: Paeoniflorin improves cardiac function and decreases adverse postinfarction left ventricular remodeling in a rat model of acute myocardial infarction. Drug Des Devel Ther. 2018, 12:823-36. 10.2147/DDDT.S163405
44. Fang X, Ji Y, Li S, et al.: Paeoniflorin attenuates cuproptosis and ameliorates left ventricular remodeling after AMI in hypobaric hypoxia environments. J Nat Med. 2024, 78:664-76. 10.1007/s11418-024-01781-7
45. Ma H, Hao J, Liu H, et al.: Peoniflorin preconditioning protects against myocardial ischemia/reperfusion injury through inhibiting myocardial apoptosis: RISK pathway involved. Appl Biochem Biotechnol. 2022, 194:1149-65. 10.1007/s12010-021-03680-z
46. Nizamutdinova IT, Jin YC, Kim JS, et al.: Paeonol and paeoniflorin, the main active principles of Paeonia albiflora, protect the heart from myocardial ischemia/reperfusion injury in rats. Planta Med. 2008, 74:14-8. 10.1055/s-2007-993775
47. Wu F, Ye B, Wu X, Lin X, Li Y, Wu Y, Tong L: Paeoniflorin on rat myocardial ischemia reperfusion injury of protection and mechanism research. Pharmacology. 2020, 105:281-8. 10.1159/000503583
48. Wu H, Zhang P, Zhou J, et al.: Paeoniflorin confers ferroptosis resistance by regulating the gut microbiota and its metabolites in diabetic cardiomyopathy. Am J Physiol Cell Physiol. 2024, 326:C724-41. 10.1152/ajpcell.00565.2023
49. Zhou H, Yang HX, Yuan Y, et al.: Paeoniflorin attenuates pressure overload-induced cardiac remodeling via inhibition of TGFβ/Smads and NF-κB pathways. J Mol Histol. 2013, 44:357-67. 10.1007/s10735-013-9491-x
50. Cao W, Zhang W, Liu J, et al.: Paeoniflorin improves survival in LPS-challenged mice through the

suppression of TNF-α and IL-1β release and augmentation of IL-10 production. Int Immunopharmacol. 2011, 11:172-8. 10.1016/j.intimp.2010.11.012

51. Wang C, Wang L, Wang L: Paeoniflorin improves autoimmune myocarditis in young rat by inhibiting CXCR5 to reduce follicular helper T cells. Autoimmunity. 2022, 55:632-9. 10.1080/08916934.2022.2128783
52. Wang S, Jia D, Lu H, Qu X: Paeoniflorin improves myocardial injury via p38 MAPK/NF-KB p65 inhibition in lipopolysaccharide-induced mouse. Ann Transl Med. 2021, 9:1449. 10.21037/atm-21-4049
53. Wang XT, Peng Z, An YY, et al.: Paeoniflorin and hydroxysafflor yellow A in xuebijing injection attenuate sepsis-induced cardiac dysfunction and inhibit proinflammatory cytokine production. Front Pharmacol. 2020, 11:614024. 10.3389/fphar.2020.614024
54. Xiao L, Xi X, Zhao M, Zhang L, Zhang K, Xu Z: Buyang huanwu decoction (BYHWD) alleviates sepsis-induced myocardial injury by suppressing local immune cell infiltration and skewing M2-macrophage polarization. Am J Transl Res. 2023, 15:2389-406. 10.2139/ssrn.4049555
55. Zhai J, Guo Y: Paeoniflorin attenuates cardiac dysfunction in endotoxemic mice via the inhibition of nuclear factor-κB. Biomed Pharmacother. 2016, 80:200-6. 10.1016/j.biopha.2016.03.032
56. Chen C, Du P, Wang J: Paeoniflorin ameliorates acute myocardial infarction of rats by inhibiting inflammation and inducible nitric oxide synthase signaling pathways. Mol Med Rep. 2015, 12:3937-43. 10.3892/mmr.2015.3870
57. Han F, Zhou D, Yin X, et al.: Paeoniflorin protects diabetic mice against myocardial ischemic injury via the transient receptor potential vanilloid 1/calcitonin gene-related peptide pathway. Cell Biosci. 2016, 6:37. 10.1186/s13578-016-0085-7
58. Liu M, Ai J, Feng J, Zheng J, Tang K, Shuai Z, Yang J: Effect of paeoniflorin on cardiac remodeling in chronic heart failure rats through the transforming growth factor β1/Smad signaling pathway. Cardiovasc Diagn Ther. 2019, 9:272-80. 10.21037/cdt.2019.06.01
59. Liu M, Feng J, Du Q, Ai J, Lv Z: Paeoniflorin attenuates myocardial fibrosis in isoprenaline-induced chronic heart failure rats via inhibiting P38 MAPK pathway. Curr Med Sci. 2020, 40:307-12. 10.1007/s11596-020-2178-0
60. Li JZ, Yu SY, Wu JH, Shao QR, Dong XM: Paeoniflorin protects myocardial cell from doxorubicin-induced apoptosis through inhibition of NADPH oxidase. Can J Physiol Pharmacol. 2012, 90:1569-75. 10.1139/y2012-140
61. Ren S, Wang Y, Zhang Y, et al.: Paeoniflorin alleviates AngII-induced cardiac hypertrophy in H9c2 cells by regulating oxidative stress and Nrf2 signaling pathway. Biomed Pharmacother. 2023, 165:115253. 10.1016/j.biopha.2023.115253
62. Shao Q, Li J, Huang X, Zhou G: Protective effects of paeoniflorin on acrolein-induced apoptosis in H9c2 cardiomyocytes. Pak J Pharm Sci. 2020, 33:1585-92. 10.36721/PJPS.2020.33.4.REG.1585-1592.1